PHYSICAL REVIEW B **78**, 020301(R) (2008)

Lattice dynamics of vanadium: Inelastic x-ray scattering measurements

Alexey Bosak,[1] Moritz Hoesch,[1] Daniele Antonangeli,[2,3] Daniel L. Farber,[2,4] Irmengard Fischer,[1] and Michael Krisch[1]
[1]*European Synchrotron Radiation Facility, Boîte Postale 220, 38043 Grenoble Cedex, France*
[2]*Lawrence Livermore National Laboratory, Livermore, California 94550, USA*
[3]*Institut de Minéralogie et de Physique des Milieux Condensés, UMR CNRS 7590, Institut de Physique du Globe de Paris, Université Paris 6 et 7, 75005 Paris, France*
[4]*University Of California, Santa Cruz, Santa Cruz, California 95064, USA*
(Received 15 April 2008; revised manuscript received 28 May 2008; published 16 July 2008)

We measured the phonon dispersions in vanadium along the principal symmetry directions using inelastic x-ray scattering. Our data complement previous results derived from thermal diffuse scattering and clearly reveal several phonon-dispersion anomalies, as well as pronounced variations of the phonon widths. Electronic structure calculations, more specifically, an analysis in terms of Fermi-surface spanning vectors allow the qualitative association of these anomalies with the topology of the Fermi surface, thus highlighting the importance of electron-phonon coupling.

DOI: 10.1103/PhysRevB.78.020301 PACS number(s): 63.20.D−, 63.20.kd, 71.15.Mb

I. INTRODUCTION

Despite decades of experimental and theoretical investigations, the physical properties of elemental transition metals are still subject of intensive research. Among the most prominent examples in the area of lattice dynamics is the search for the fingerprints of electronic topological transitions[1] in metals with hexagonal-close-packed (hcp) structure (Zn, Cd, and Os). These topological transitions are associated with changes of the Fermi-surface topology and lead to anomalies in thermodynamic and elastic properties. Another example is the high superconducting temperature of the group V*B* elements Nb(T_c=9.25 K) and V(T_c=5.3 K), which display a marked increase in T_c with pressure, anomalies which can be related to electron-phonon coupling and Fermi-surface properties.[2–4] Although both V and Nb were believed to maintain their body-centered-cubic (bcc) structures up to several hundreds of GPa, a recent x-ray diffraction study of V reported a rhombohedral lattice distortion between 63 and 69 GPa without a discontinuity in the equation of state,[5] in the same pressure range where a small anomaly in the T_c evolution was observed.[4] Lattice dynamics calculations suggest that this lattice distortion is derived from a shear instability due to a transverse phonon-mode softening arising from intraband nesting of the Fermi surface around a quarter along the Γ-H direction.[6–8] However, these computational results are still in need of experimental validation. While the phonon-dispersion curves of group V elements niobium[9–11] and tantalum[12,13] have been determined by inelastic neutron scattering (INS), data for vanadium are scarce. This is due to the fact that vanadium is essentially an incoherent scatterer, rendering conventional neutron triple axis spectrometry extremely difficult,[14] and only the generalized phonon density of states (PDOS) could be measured in a straightforward way.[5,15,16] However, using the thermal diffuse scattering (TDS) of x rays, Colella and Batterman[17] performed a remarkable study of the vanadium lattice dynamics. They reconstructed all the phonon branches and were able to resolve the existing controversies regarding an irregular behavior in the low-energy part of the acoustic phonon dispersion as well as a high-energy feature. However, due to the flux limitations of conventional x-ray tubes, the data quality did not allow for the detailed resolution of any phonon-dispersion anomalies. Nowadays, thanks to the availability of bright x-ray sources at synchrotron-radiation facilities and powerful area detectors, TDS patterns can now be recorded with excellent statistics in a few minutes but surprisingly, a recent synchrotron based TDS study devoted to vanadium[18] did not bring forth any new information on the lattice dynamics.

In the present work, we present a detailed determination of the phonon dispersions of vanadium by inelastic x-ray scattering (IXS). In contrast to the work of Ding *et al.*,[18] we identified previously undetected phonon anomalies that bear a close resemblance to anomalies previously observed in Nb and Ta that are associated with phonon line width broadening and specific features of the Fermi surface.

II. EXPERIMENTAL AND COMPUTATIONAL DETAILS

The IXS experiment was performed on beamline ID28 at the European Synchrotron Radiation Facility. The instrument was operated at 17 794 eV, providing an overall energy resolution of 3.0 meV full width at half maximum (FWHM). Direction and size of the momentum transfer were selected by an appropriate choice of the scattering angle and the sample orientation in the horizontal scattering plane. The momentum resolution was typically set to 0.28 and 0.84 nm^{-1} in the horizontal and vertical plane. The dimensions of the focused x-ray beam were 250×60 μm^2 (horizontal$\times$vertical, FWHM). Further details of the experimental setup can be found elsewhere.[19] The V single crystal was purchased from MaTecK GmbH and had well-oriented, polished (100), (110), and (111) surfaces. Typical rocking curve widths were in the order of 0.02^0. The experiment was performed in reflection geometry, and a list of measured branches together with the measurement configuration is given in Table I.

Figure 1 shows representative IXS spectra along the [0 0 1] direction. The spectra are characterized by a moderate

TABLE I. Experimental configurations for measured dispersion branches

Branch	Momentum transfer	Propagation	Polarization
LA [1 0 0]	[0 0 2+ξ] ($0<\xi\leq 1$)	[0 0 1]	$\langle 0\ 0\ 1\rangle$
TA [1 0 0]	[2 2 ξ] ($0<\xi\leq 1$)	[0 0 1]	$\langle 1\ 1\ 0\rangle$
LA [1 1 1]	[2−ξ 2−ξ 2−ξ] ($0<\xi\leq 1$)	[1 1 1]	$\langle 1\ 1\ 1\rangle$
TA [1 1 1]	[2−ξ 2−ξ 2+ξ] ($0<\xi\leq 1$)	[1 1 1]	$\langle 1\ 1\ -2\rangle$
LA [1 1 0]	[1+ξ 1+ξ 0] ($0<\xi\leq 0.5$)	[1 1 0]	$\langle 1\ 1\ 0\rangle$
TA $[1\ 1\ 0]_{\langle 1-1\ 0\rangle}$	[2+ξ 2−ξ 0] ($0<\xi\leq 0.5$)	[1 1 0]	$\langle 1\ -1\ 0\rangle$
TA $[1\ 1\ 0]_{\langle 0\ 0\ 1\rangle}$	[1+ξ 1+ξ 2] ($0<\xi<0.5$)	[1 1 0]	$\langle 0\ 0\ 1\rangle$

elastic contribution centered at zero energy and two symmetric features: the Stokes and anti-Stokes peaks of the corresponding phonons. The energy position $E(q)$ and width of the phonons were extracted using a model function composed of a sum of Lorentzian functions, for which the inelastic contributions were constrained by the Bose factor. This model function was then convoluted with the experimentally determined resolution function and fitted to the IXS spectra, utilizing a standard χ^2 minimization routine. The half width at half maximum (HWHM) extracted from this function can be considered to be reliable only for values larger than 0.3 meV, corresponding to 1/5 of the width of the resolution function.

Ab initio calculations of the Fermi surface (FS) of V and Nb were performed using the WIEN2K code.[20] The electronic ground state was converged in a 27^3 grid reduced to the irreducible wedge of momentum space using the generalized gradient approximation (GGA) and standard parameters. The FS was represented by integrating the eigenvalues over ± 18 meV around the Fermi level E_F to yield a function that is unity at the Fermi wave vector and decays rapidly as the electronic bands disperse away from E_F. To discuss the nesting properties of the FS, the density of spanning vectors was calculated as the periodic autocorrelation of this FS function.[21] This density of spanning vectors thus naturally diverges at zero momentum (Γ point) and shows features where the spanning condition is fulfilled between different sheets or within a sheet of the Fermi surface. Due to the complex nature of the *d*-band topology, the features for V and Nb are not very pronounced, yet some can be assigned to specific nesting geometries. Their correspondence to anomalies observed in the phonon dispersions is discussed in Sec. III.

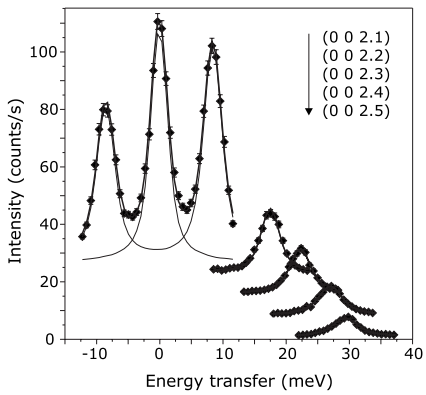

FIG. 1. Selected IXS spectra for the LA [1 0 0] branch at the indicated Q values (given in reciprocal-lattice vector components). The experimental data are shown together with the best fit results (thin solid lines for the individual components and solid lines for the total fit). The spectra are shifted in the vertical direction for clarity, conserving the same intensity scale. The counting time per point was between 15 and 45 s.

III. RESULTS AND DISCUSSION

We measured all the phonon branches along high-symmetry directions [Fig. 2(a)]. The long-wavelength part of the dispersion shows an excellent fit with the elastic moduli measured by ultrasonic pulse-echo technique.[22] The phonon dispersions derived from the earlier TDS study[8] are overall in remarkable agreement with our IXS results [Fig. 2(b)]. In

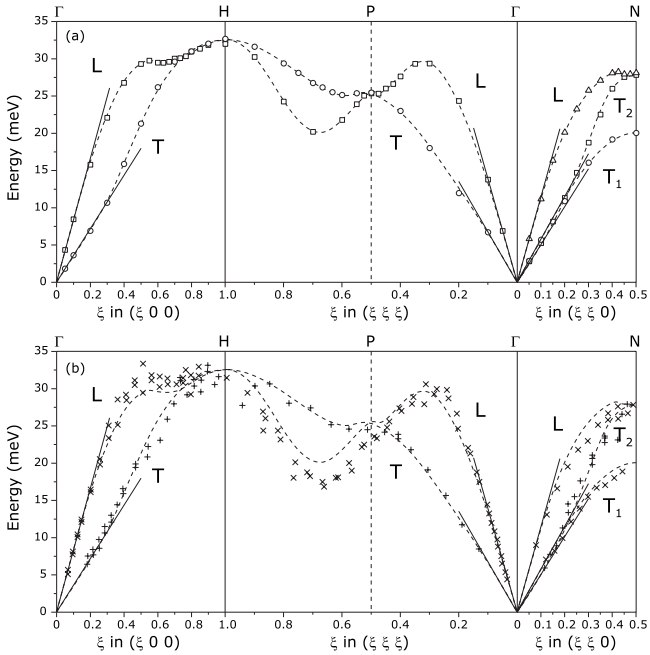

FIG. 2. Phonon dispersion for vanadium along high-symmetry directions: (a) experimental points, together with guides to the eye (dashed Bézier curves); solid lines correspond to the long-wavelength limit from ultrasonic measurements (Ref. 12) and (b) comparison of our experimental dispersion (dashed lines) with thermal diffuse scattering data (Ref. 8).

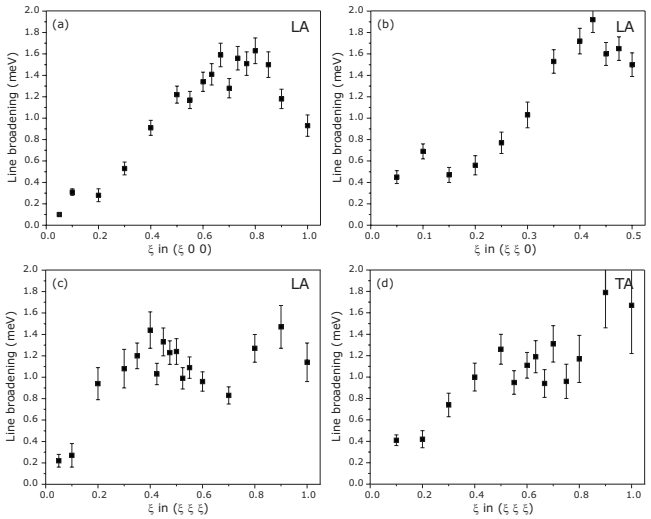

FIG. 3. Line broadening (HWHM) for LA phonons along the (a)Γ-*H*, (b)Γ-*N*, and (c)Γ-*P*-*H* directions and TA phonons along the (d)Γ-*P*-*H* direction.

particular, the anomalous upward bending of the TA[100] and TA_2[110] branches is well reproduced. Substantial deviations to the TDS result occur only for longitudinal phonons propagating along the ⟨1 1 1⟩ direction. Furthermore, the anomaly of the LA[100] branch for $0.55 < x < 0.9$ and the overbending of the LA[110] branch are clearly revealed in the present IXS study. A comparison with the results of Ref. 18 is difficult since the published data set is incomplete (no data for the Γ-*H* direction and no transverse branches for the Γ-*N* direction). It appears, though, that the reported subset of phonon branches does not contain more information than the original work of Colella and Batterman.[17]

In addition to the phonon energies, we carefully studied the phonon linewidths for LA phonons propagating along the Γ-*H* and Γ-*N* directions. The phonon widths, reported in Fig. 3, were obtained from the IXS spectra by fitting the model function convoluted with the experimental resolution function as described above.

A strong increase in the phonon width up to 1.8 meV HWHM is observed in the ξ region where the phonon branches show deviations from the normal behavior. It is worth noting that the relatively weak overbending of the LA branch close to the *N* point manifests itself in a very strong phonon broadening.

The dispersion anomalies reveal themselves either as deviations from a fictional "noninteracting" lattice dynamics (softening) or as increased width of the phonon lines, or as a combination of both. The noninteracting dispersion is shown in Fig. 4 as a two-neighbor lattice dynamics model, therefore excluding any long-range forces. The anomalies for V, highlighted by the direct comparison of the noninteracting dispersion model with the experimental dispersion (Fig. 4) can be summarized as follows: (1) TA phonon along Γ-*H* around ξ=0.24. The anomalous upward bending is enhanced by a softening. This was previously assigned to a specific intraband Fermi-surface nesting.[7] (2) LA phonon close to *H* along Γ-*H*. A broad and very pronounced softening is observed

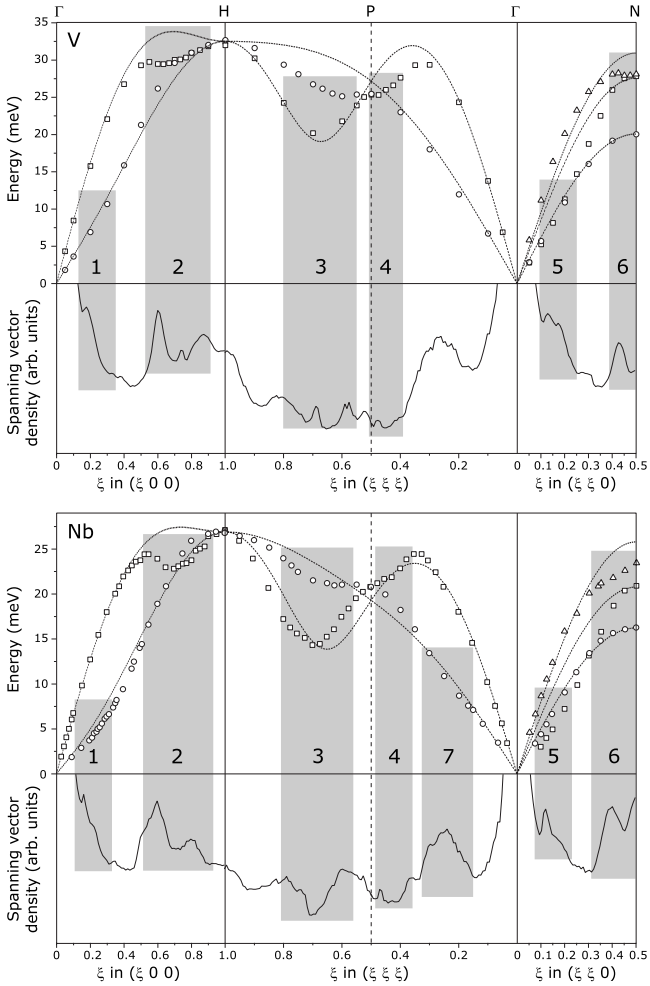

FIG. 4. Phonon dispersions in vanadium and niobium (Ref. 9) compared to the FS spanning vector density (see text). The numbered shaded areas are guides to the eye associated with anomalies. The dashed lines correspond to a two-neighbor lattice dynamics model that mimics the phonon dispersion without long-range interactions. The energy scale is not retained for the Γ-*N* direction.

along with a distinct broadening at ξ=0.8 [Fig. 3(a)]. (3). The TA phonon along *H*-*P* deviates from a sinusoidal dispersion over a very broad range along ($\xi\xi\xi$), most pronounced for $0.55 < \xi < 0.8$; substantial broadening is observed in a wide ξ range [Fig. 3(d)]. (4) Close to the *P* point along Γ-*P*, the *L* phonon shows a strong overbending that leads to a plateau around the *P* point with a broadening at ξ=0.4 [Fig. 3(c)]. (5) Similar to (1), the TA1 phonon is decreased along Γ-*N*, leading to a reduction in the speed of sound and a parabolic component in the dispersion. (6) Very close to the *N* point a weak dip in the dispersion is observed. This slight anomaly finds its counterpart in a strong broadening of the phonon linewidth [Fig. 3(b)] with a maximum at ξ=0.42.

Inspection of the previously published data for Nb (Ref. 9) reveals essentially the same anomalies. In addition to the above mentioned, a dip in the dispersion along Γ-*P* is marked as (7) in Fig. 4(b). Our data for V [Fig. 4(a)] show a similar dip, but the density of data points is not sufficient along this branch to resolve it in detail. Also for Ta the phonon dispersion from an INS data set[12,13] shows anomalies at

the same or similar momentum space regions. The data points are, however, not dense enough to well localize the dispersion anomalies other than along the Γ-*H* direction. We therefore did not include them in our comparison and discussion below.

To further shed light on the observed phonon anomalies, we performed calculations of the electronic structure, the Fermi surface, and in particular the density of Fermi-surface spanning possibilities in momentum space. The results are reported in the lower parts of Figs. 4(a) and 4(b) for V and Nb, respectively. Features of this FS spanning vector density that correspond to the observed anomalies are marked as gray bars. Due to the complex topography of the *d*-band FS that offers many spanning opportunities,[23] the assignment of features to specific nesting conditions is mostly not possible. The FS spanning density naturally diverges at small momentum close to Γ and the features are observed on top of a smooth decaying background of this divergence. For V we can assign anomaly (1) to a shoulder close to Γ that decays sharply at the position where the anomaly is most pronounced. Anomaly (2) starts at a sharp peak and corresponds to a region of high spanning density. The width of anomaly (3) does not allow attributing it reliably to a specific spanning feature. Anomaly (4) again corresponds to the sharp decay of the spanning density and thus, apparently, to an extremal spanning condition of the FS. Anomaly (5) is, similar to anomaly (1), a shoulder on the decay away from Γ, and anomaly (6) is well reproduced in the FS spanning density as a sharp peak. Anomaly (7) cannot be localized for vanadium as the density of experimental points is not sufficient but should presumably exist, being associated with a large spanning density peak as for niobium.

IV. CONCLUSIONS

In summary, we determined the complete phonon-dispersion relation of vanadium by IXS. The data are in good agreement with the previously reported TDS results. Our *ab initio* calculations of the Fermi surface show an overall good correlation with the positions of phonon-dispersion anomalies, emphasizing the importance of electron-phonon coupling.[10,24]

These results complete the existing data on the lattice dynamics of group V transition metals and provide an important benchmark for future experimental studies and theoretical advances. More specifically, our IXS results and related calculations at ambient pressure form an important basis for future high-pressure studies aiming at validating the predicted transverse phonon branch softening related to the structural phase transition and the anomaly in the superconducting temperature.[25] More generally, studies of phonon dispersions under high pressure can provide solid validations of theoretical predictions and today, the actual capacities of the IXS technique[26] make such experiments feasible.

[1] I. M. Lifshitz, Zh. Eksp. Teor. Fiz. **38**, 1569 (1960) [Sov. Phys. JETP **11**, 1130 (1960)].
[2] V. V. Struzhkin, Y. A. Timofeev, R. J. Hemley, and H.-K. Mao, Phys. Rev. Lett. **79**, 4262 (1997).
[3] J. S. Tse, Z. Li, K. Uehara, Y. Ma, and R. Ahuja, Phys. Rev. B **69**, 132101 (2004).
[4] M. Ishizuka, M. Iketani, and S. Endo, Phys. Rev. B **61**, R3823 (2000).
[5] Y. Ding, R. Ahuja, J. Shu, P. Chow, W. Luo, and H.-K. Mao, Phys. Rev. Lett. **98**, 085502 (2007).
[6] N. Suzuki and M. Otani, J. Phys.: Condens. Matter **14**, 10869 (2002).
[7] A. Landa, J. Kelpeis, P. Soderlind, I. Naumov, O. Velikokhatnyi, L. Vitos, and A. Ruban, J. Phys.: Condens. Matter **18**, 5079 (2006).
[8] N. Suzuki and M. Otani, J. Phys.: Condens. Matter **19**, 125206 (2007).
[9] Y. Nakagawa and A. D. B. Woods, Phys. Rev. Lett. **11**, 271 (1963).
[10] R. I. Sharp, J. Phys. C **2**, 421 (1969).
[11] R. I. Sharp, J. Phys. C **2**, 432 (1969).
[12] A. D. B. Woods, Phys. Rev. **136**, A781 (1964).
[13] F. Sacchetti, C. Petrillo, and O. Moze, Phys. Rev. B **49**, 8747 (1994).
[14] A. S. Ivanov and A. Yu. Rumiantsev, Physica B **276-278**, 197 (2000).
[15] C. M. Eisenhauer, I. Pelah, D. J. Hughes, and H. Palevsky, Phys. Rev. **109**, 1046 (1958).
[16] D. J. Page, Proc. Phys. Soc. London **91**, 76 (1967).
[17] R. Colella and B. W. Batterman, Phys. Rev. B **1**, 3913 (1970).
[18] Y. Ding, P. Chow, H.-K. Mao, Y. Ren, and C. T. Prewitt, Appl. Phys. Lett. **88**, 061903 (2006).
[19] M. Krisch and F. Sette, in *Light Scattering in Solids, Novel Materials and Techniques*, Topics in Applied Physics No. 108 (Springer-Verlag, Berlin, 2007).
[20] P. Blaha, K. Schwarz, G. K. H. Madsen, D. Kvasnicka, and J. Luitz, *Wien2k, An Augmented Plane Wave Plus Local Orbitals Program for Calculating Crystal Properties* (Karlheinz Schwarz, Techische Universitat Wien, Austria, 2001).
[21] In a regular grid (*gij*) that obeys the cubic symmetry, the Fermi surface is represented as $F_{gij}=\Sigma_n \exp[-(E_{gij}^{(n)}-E_F)^2/2\sigma^2]$, where $E_{gij}^{(n)}$ are all electronic eigenvalues and $\sigma=35$ meV is the integration window. The density of spanning vectors is $D_{hkl}=\Sigma_{gij}[F_{gij}\cdot F_{(g+h,j+k,j+l)_{\mathrm{mod}}}]$, where the sum runs over the same cubic grid with indices modulo the size of the unit cell in the reciprocal space.
[22] G. A. Alers, Phys. Rev. **119**, 1532 (1960).
[23] See EPAPS Document No. E-PRBMDO-78-R11826 for the visualization of the contributions to the spanning density for selected momentum transfers. For more information on EPAPS, see http://www.aip.org/pubservs/epaps.html.
[24] B. M. Powell, P. Martel, and A. D. B. Woods, Phys. Rev. **171**, 727 (1968).
[25] Y. Ding, R. Ahuja, J. Shu, P. Chow, W. Luo, and H. K. Mao, Phys. Rev. Lett. **98**, 085502 (2007).
[26] D. L. Farber, M. Krisch, D. Antonangeli, A. Beraud, J. Badro, F. Occelli, and D. Orlikowski, Phys. Rev. Lett. **96**, 115502 (2006).